

## Supporting Information

### “Tandem-action” Ferrocenyl Iodocuprates Promoting Low Temperature Hypergolic Ignitions of “Green” EILs-H<sub>2</sub>O<sub>2</sub> Bipropellants

Kangcai Wang,<sup>a</sup> Tianlin Liu,<sup>a</sup> Yunhe Jin,<sup>a</sup> Huang Shi,<sup>a</sup> Natan Petrutik,<sup>b</sup> Daniel Shem-Tov,<sup>b</sup>

Qi-Long Yan,<sup>c\*</sup> Michael Gozin<sup>b\*</sup> and Qinghua Zhang<sup>a\*</sup>

#### Table of content

Materials and Methods.....	S2
<sup>1</sup> H NMR and <sup>13</sup> C NMR Spectra.....	S2-S5
IR Spectra.....	S6
Crystallographic data for promoters <b>P1</b> , <b>P2</b> and <b>P4</b> .....	S7
X-Ray Structure of promotor <b>P4</b> .....	S7
Powder XRD of promoters <b>P1</b> and <b>P2</b> .....	S8
Accelerated stability studies of EIL fuel-promoter formulations .....	S9- S10
Heats of formation.....	S11-S12

## Materials and Methods

All reagents were obtained from commercial resources were used as received.  $^1\text{H}$  and  $^{13}\text{C}$  NMR spectra were measured on Bruker AV II-400 MHz spectrometer, using  $\text{DMSO-d}_6$  as solvents. Single-crystal data were collected on an Oxford Xcalibur diffractometer with a CCD detector  $\text{Mo-K}\alpha$  radiation ( $\lambda = 0.71073 \text{ \AA}$ ), using a  $\omega$  scan for promoters **P1** and **P2** at  $173 \text{ }^\circ\text{C}$ . The direct method and full-matrix least-squares method on **F2** contained in the SHELXTL program package were used to resolve and refine the structures. Crystallographic data of promoters **P1** and **P2** are shown in Table S1. Powder X-ray diffractions (PXRD) were carried out on Rigaku D/MAX-rA diffractometers using  $\text{Cu-K}\alpha$  radiation. FTIR (ATR) spectra were recorded on a Nicolet impact 410 FTIR spectrometer. Densities were measured on AccuPyc II 1345 Series Pycnometer apparatus. Viscosities were measured by Brookfield DV3T Rheometer.

## $^1\text{H}$ NMR and $^{13}\text{C}$ NMR Spectroscopy

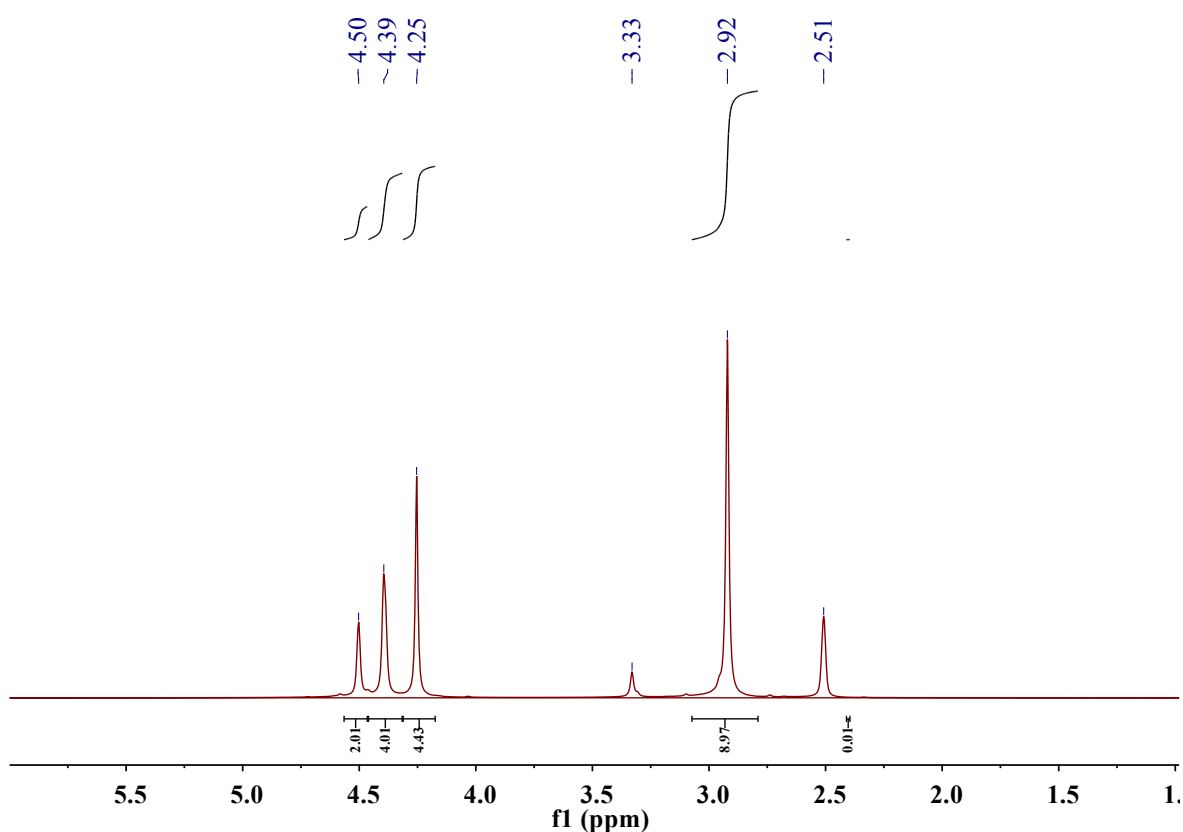


**Figure S1.**  $^1\text{H}$  NMR (400 MHz,  $\text{DMSO-d}_6$ ) of promoter **P1**.

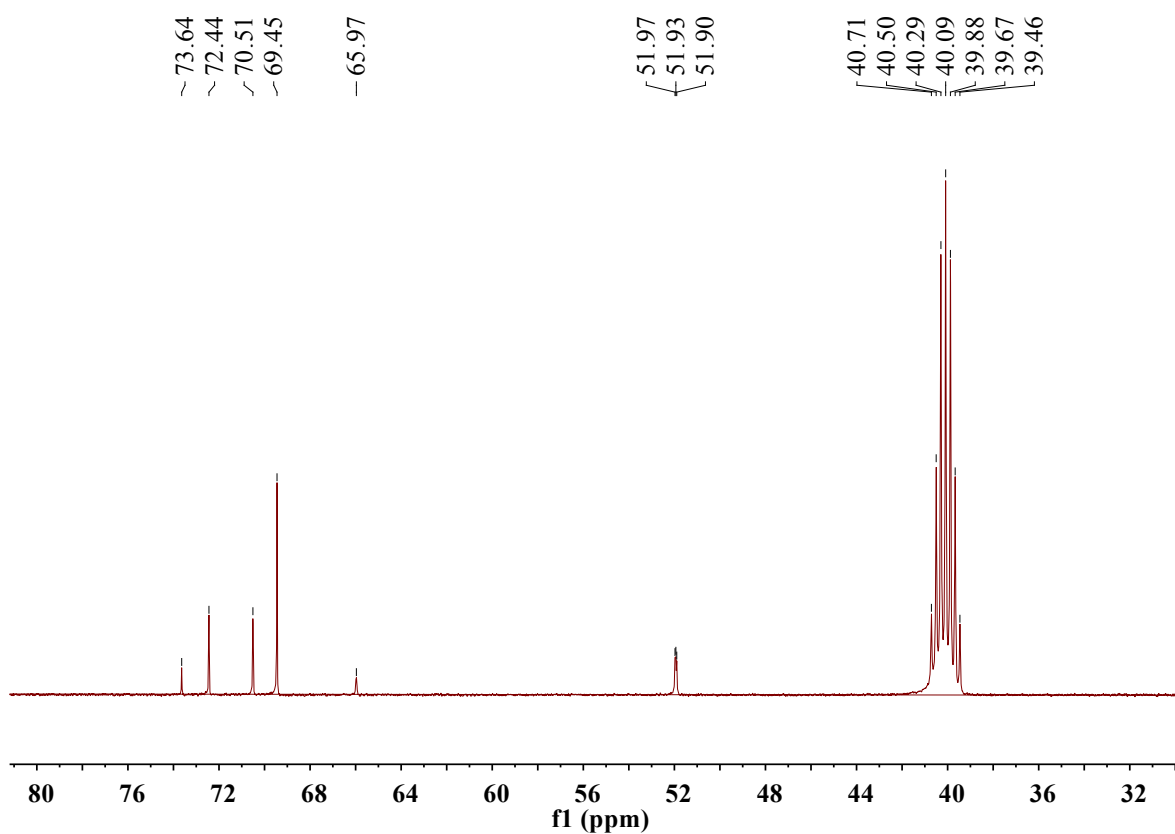


**Figure S2.**  $^{13}\text{C}$  NMR (100 MHz,  $\text{DMSO-d}_6$ ) of promoter **P1**.

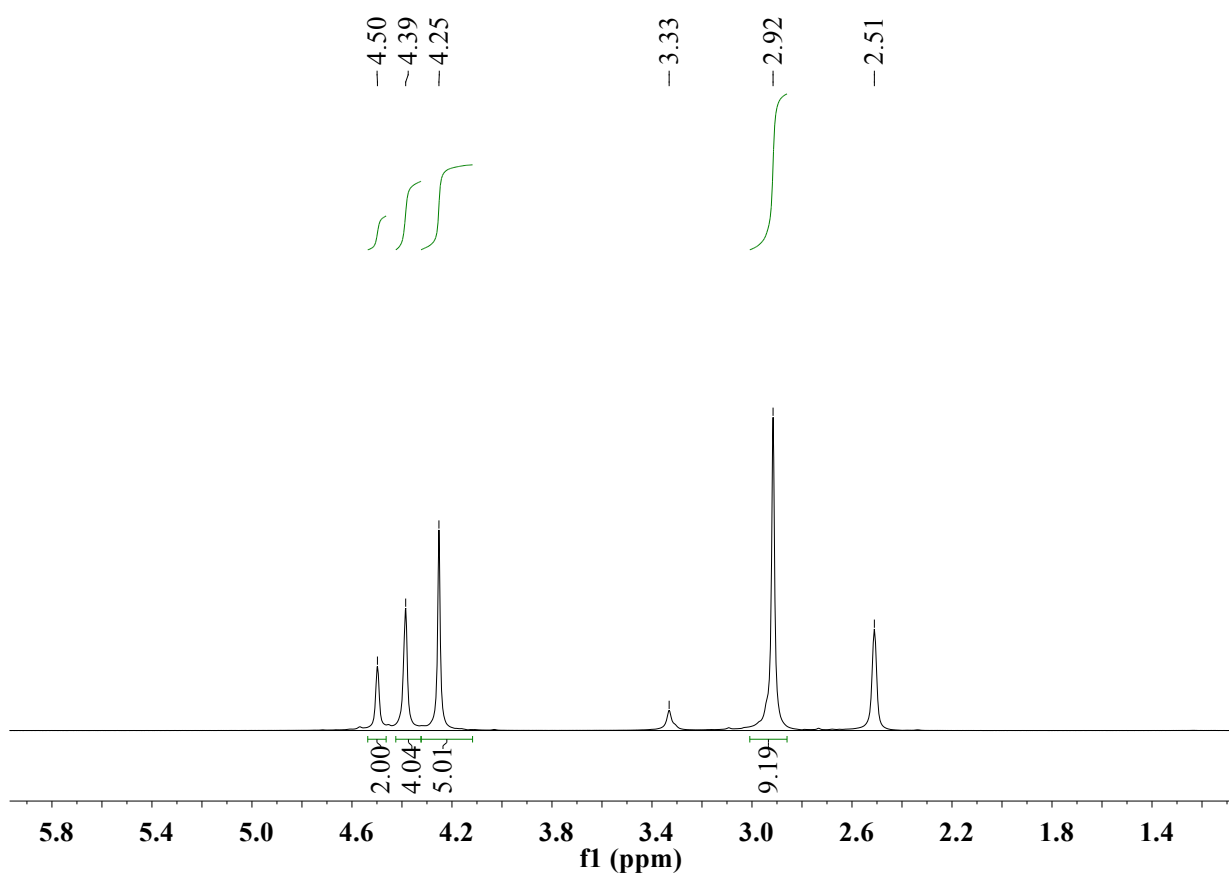


**Figure S3.**  $^1\text{H}$  NMR (400 MHz,  $\text{DMSO-d}_6$ ) of promoter **P2**.

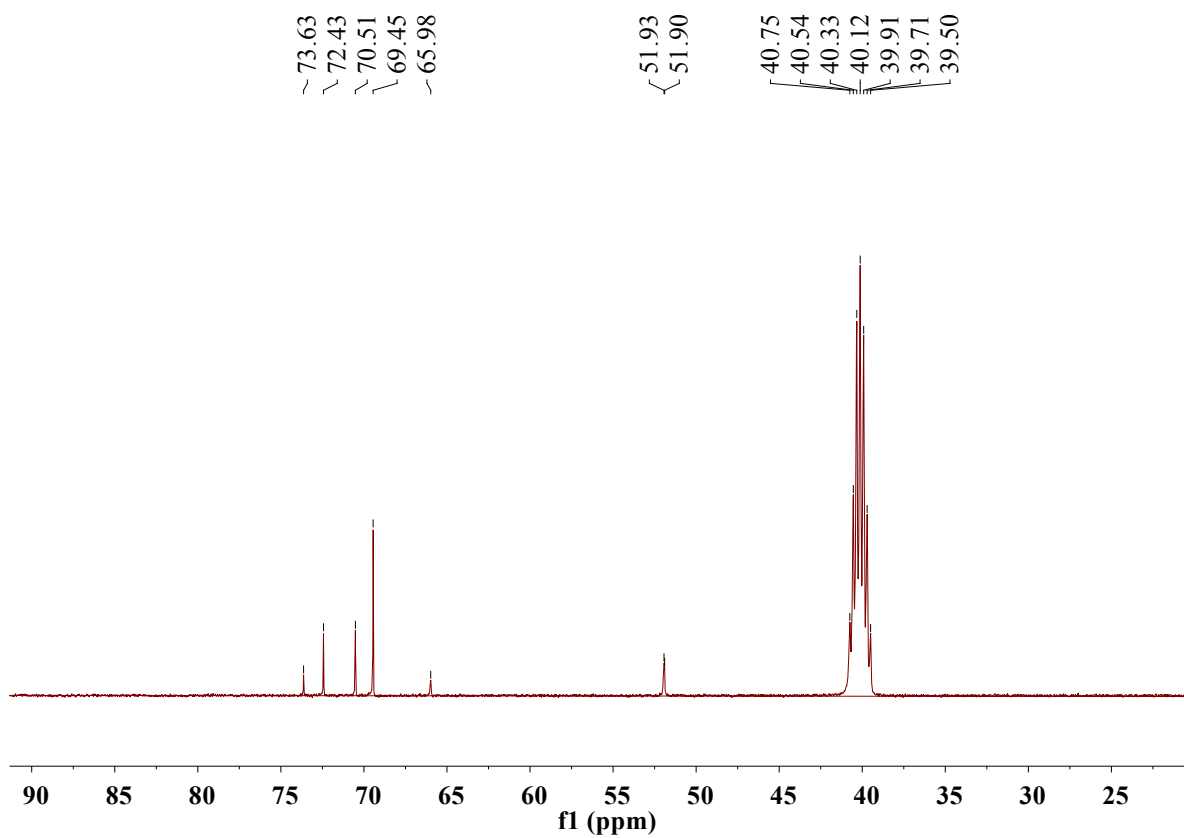


**Figure S4.**  $^{13}\text{C}$  NMR (100 MHz,  $\text{DMSO-d}_6$ ) of promoter **P2**.

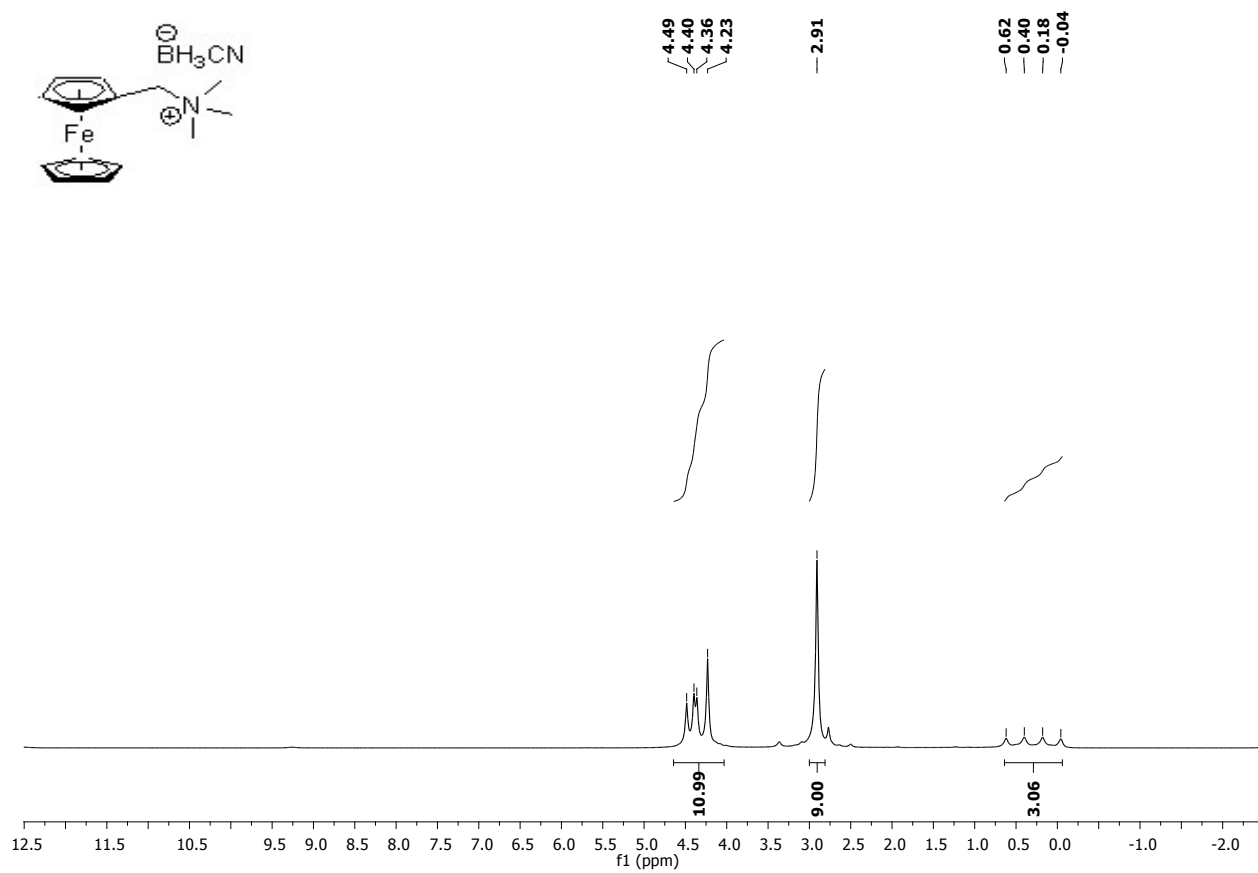


**Figure S5.**  $^1\text{H}$  NMR (400 MHz,  $\text{DMSO-d}_6$ ) of promoter **P3**.

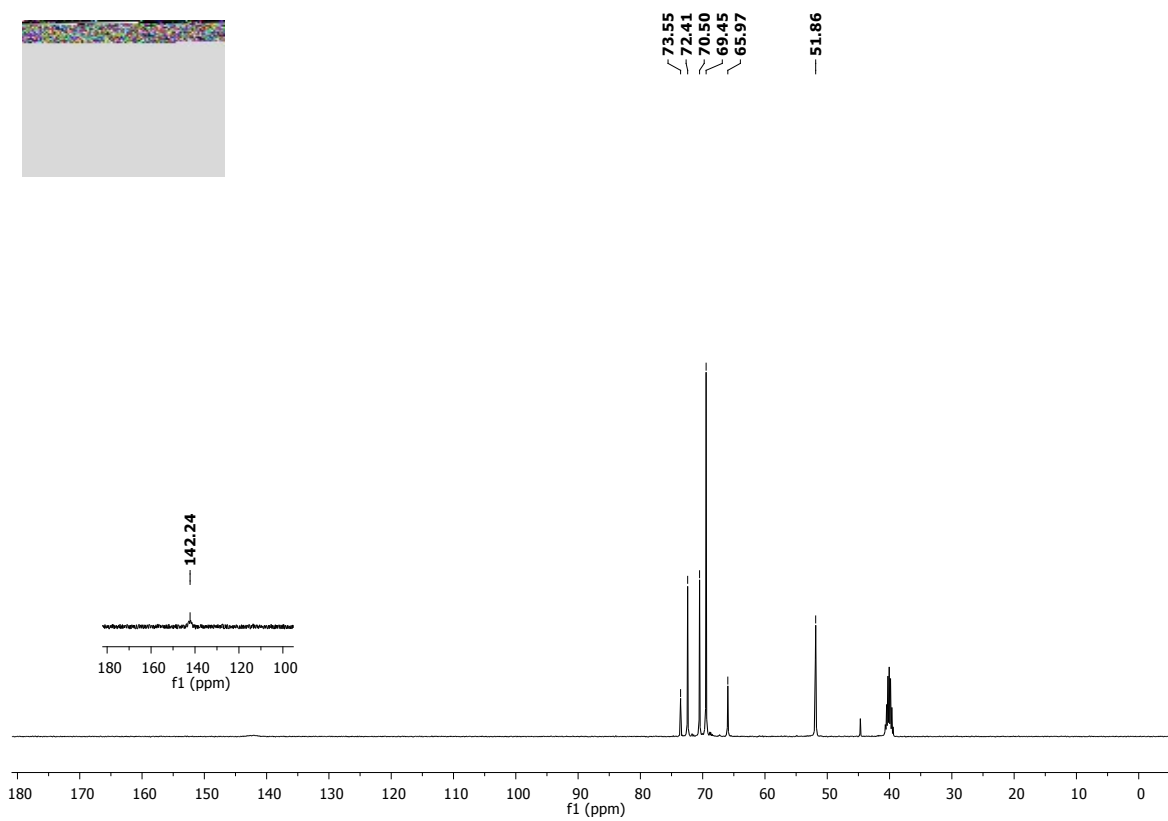


**Figure S6.** <sup>13</sup>C NMR (100 MHz, DMSO-d<sub>6</sub>) of promoter **P3**.

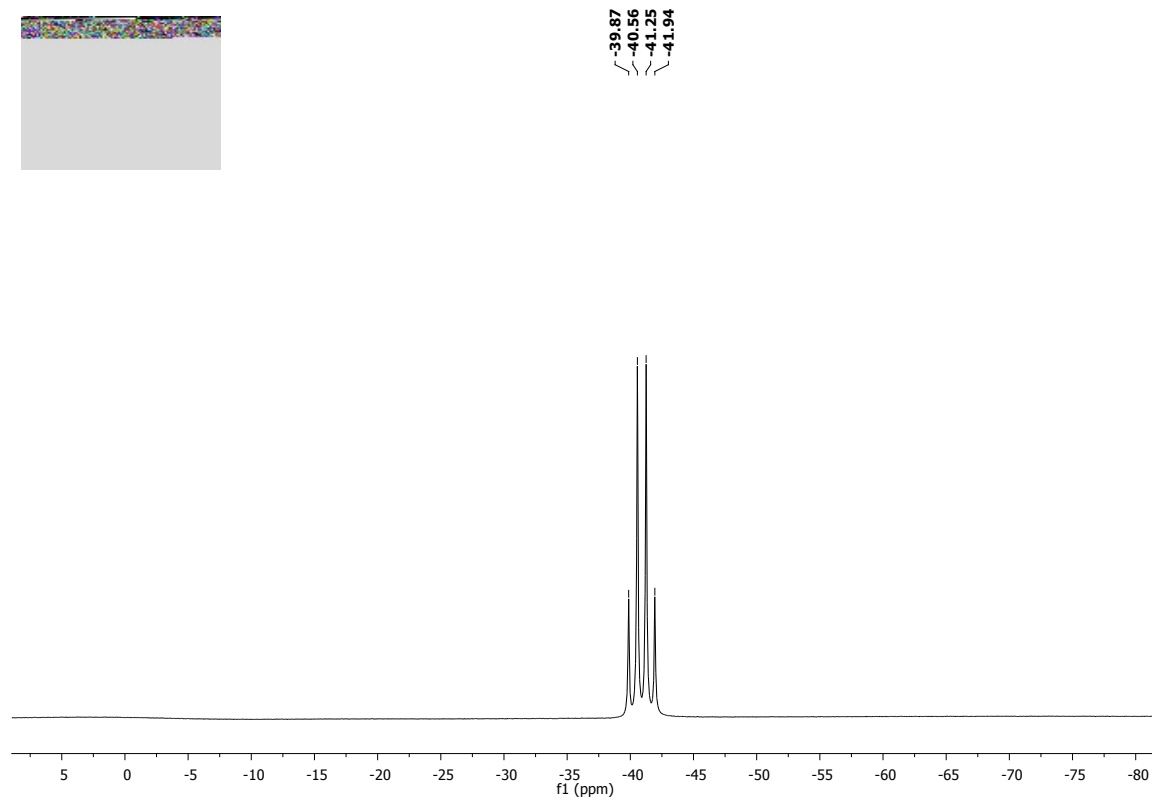


**Figure S7.** <sup>11</sup>B NMR (128 MHz, DMSO-d<sub>6</sub>) of promoter **P3**.

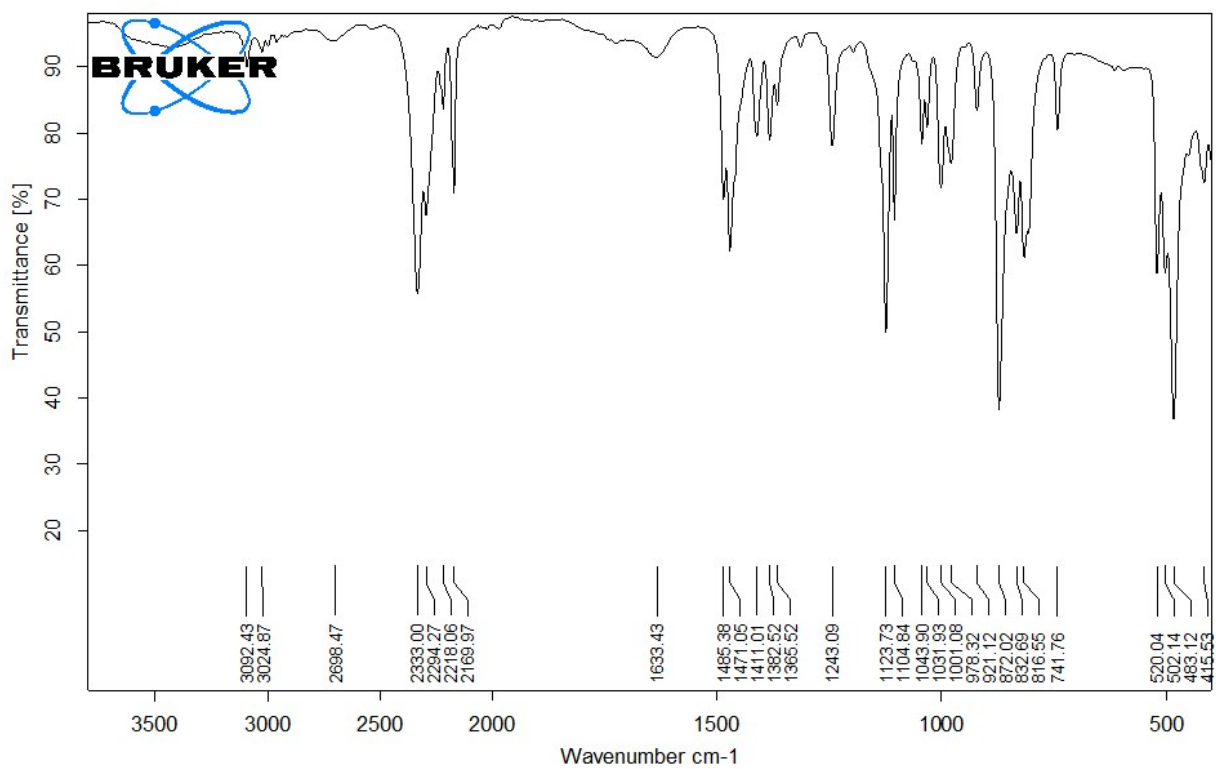


**Figure S8.** IR (ATR) of promoter **P3**.

**Table S1.** Crystallographic data for promoters **P1**, **P2** and **P4**.

	<b>Promoter P1</b> (CCDC 1986753)	<b>Promoter P2</b> (CCDC 1986752)	<b>Reference Promoter P4</b> (CCDC 2000609)
Formula	C <sub>14</sub> H <sub>20</sub> NCuFeI <sub>2</sub>	C <sub>28</sub> H <sub>40</sub> N <sub>2</sub> Cu <sub>4</sub> Fe <sub>2</sub> I <sub>6</sub>	C <sub>7</sub> H <sub>18</sub> Cu <sub>2</sub> I <sub>3</sub> N
FW/g·mol <sup>-1</sup>	575.50	1531.88	624.00
Crystal system	monoclinic	monoclinic	monoclinic
Space group	<i>P2</i> <sub>1</sub> / <i>c</i>	<i>P2</i> <sub>1</sub>	<i>P 2</i> <sub>1</sub> / <i>c</i>
a/Å	11.0739 (13)	8.3061 (15)	8.4030 (1)
b/Å	10.4449 (12)	9.6795 (16)	10.4933 (1)
c/Å	15.2751 (17)	24.4790 (14)	17.5405 (2)
α°	90	90	90
β°	94.19 (2)	94.855 (4)	91.559 (1)
γ°	90	90	90
V/Å <sup>3</sup>	1762.1 (3)	1961.1 (6)	1546.07 (3)
ρ <sub>calcd.</sub> /g·mol <sup>-3</sup>	2.169	2.594	2.681
T/K	173	173	293
F(000)	1088.0	1416.0	1136.0
μ/mm <sup>-1</sup>	5.521	7.595	50.154
h, k, l	-14<h<13, -13<k<13, -19<l<19	-9<h<9, -10<k<11, -29<l<29	-9<h<10, -13<k<13, -22 <l<22
2θ range°	3.688 to 55.096	4.528 to 50.246	9.824 to 155.154
R (I>2σ)	R <sub>1</sub> =0.0397, wR <sub>2</sub> =0.0694	R <sub>1</sub> =0.0472, wR <sub>2</sub> =0.1204	R <sub>1</sub> =0.0546, wR <sub>2</sub> = 0.1621
wR <sub>2</sub> (all data)	R <sub>1</sub> =0.0625, wR <sub>2</sub> =0.0776	R <sub>1</sub> =0.0537, wR <sub>2</sub> =0.1281	R <sub>1</sub> = 0.0634, wR <sub>2</sub> = 0.1706

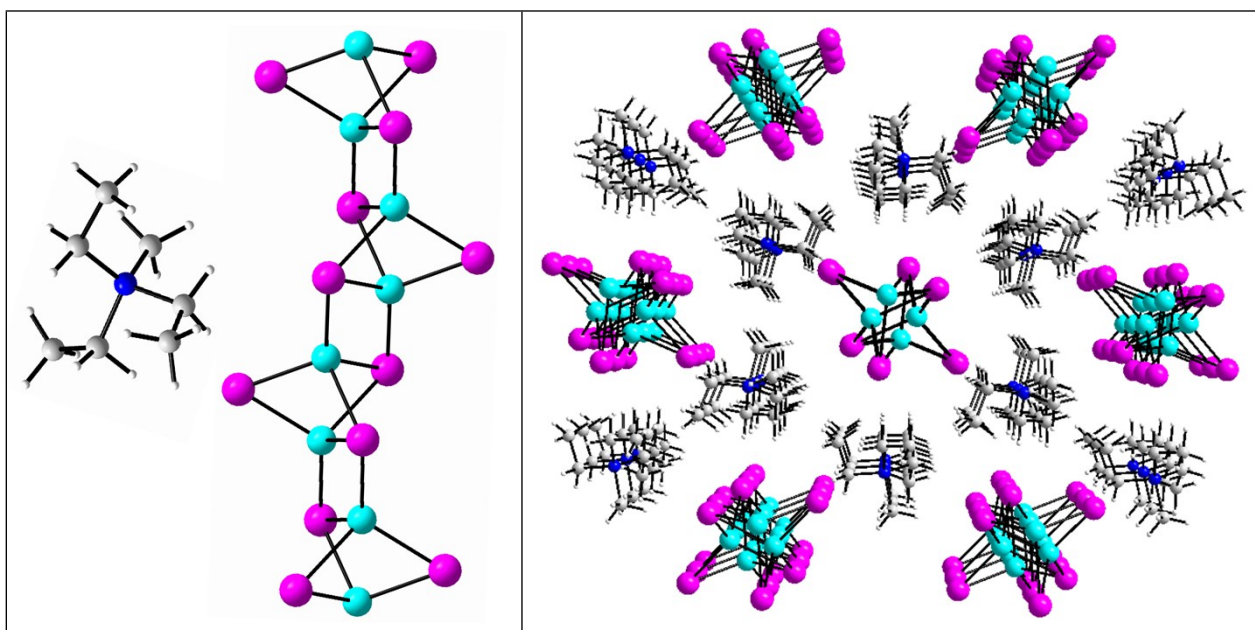


**Figure S9.** (*left*): Molecular structure of reference promoter **P4** containing  $[\text{CH}_3\text{N}(\text{CH}_2\text{CH}_3)_3]^+$  cation and  $[\text{Cu}_2\text{I}_3]^-_n$  polymeric anion; (*right*): arrangement of cations and anions in a crystal structure of reference promoter **P4** along  $[100]$  direction.

**Powder XRD**

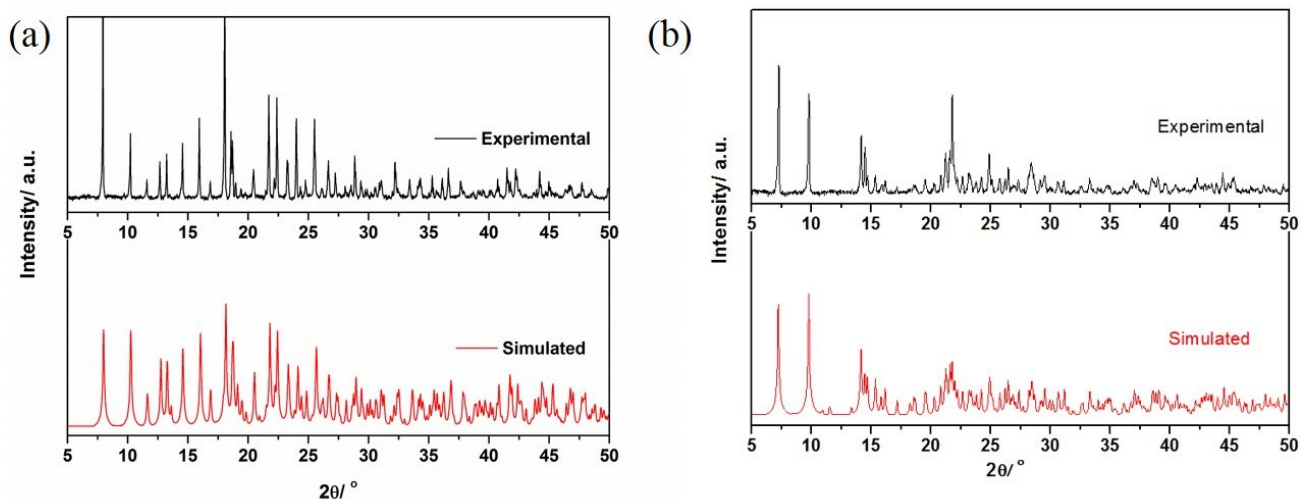


**Figure S10.** Simulated and experimental PXRD patterns. (a) promoter **P1**; (b) promoter **P2**.



## Accelerated Stability Studies of EIL Fuel-Promoter Formulations

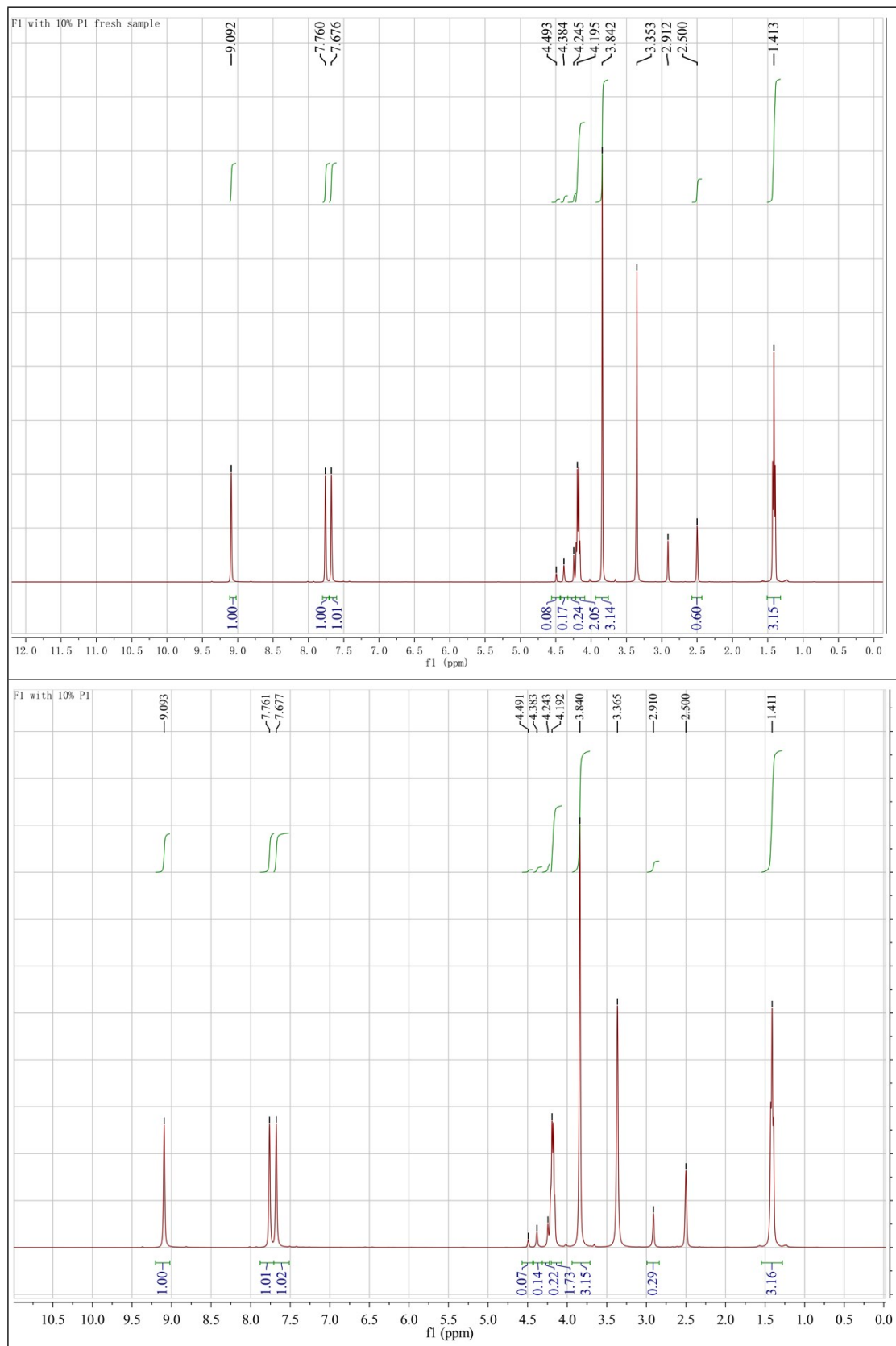


**Figure S11.** <sup>1</sup>H NMR (DMSO-d<sub>6</sub>) of EIL fuel **F1** with 10 wt.% of promoter **P1**. (*top*): Before [t<sub>0</sub>] and (*bottom*): after heating at 50°C for 7 days.

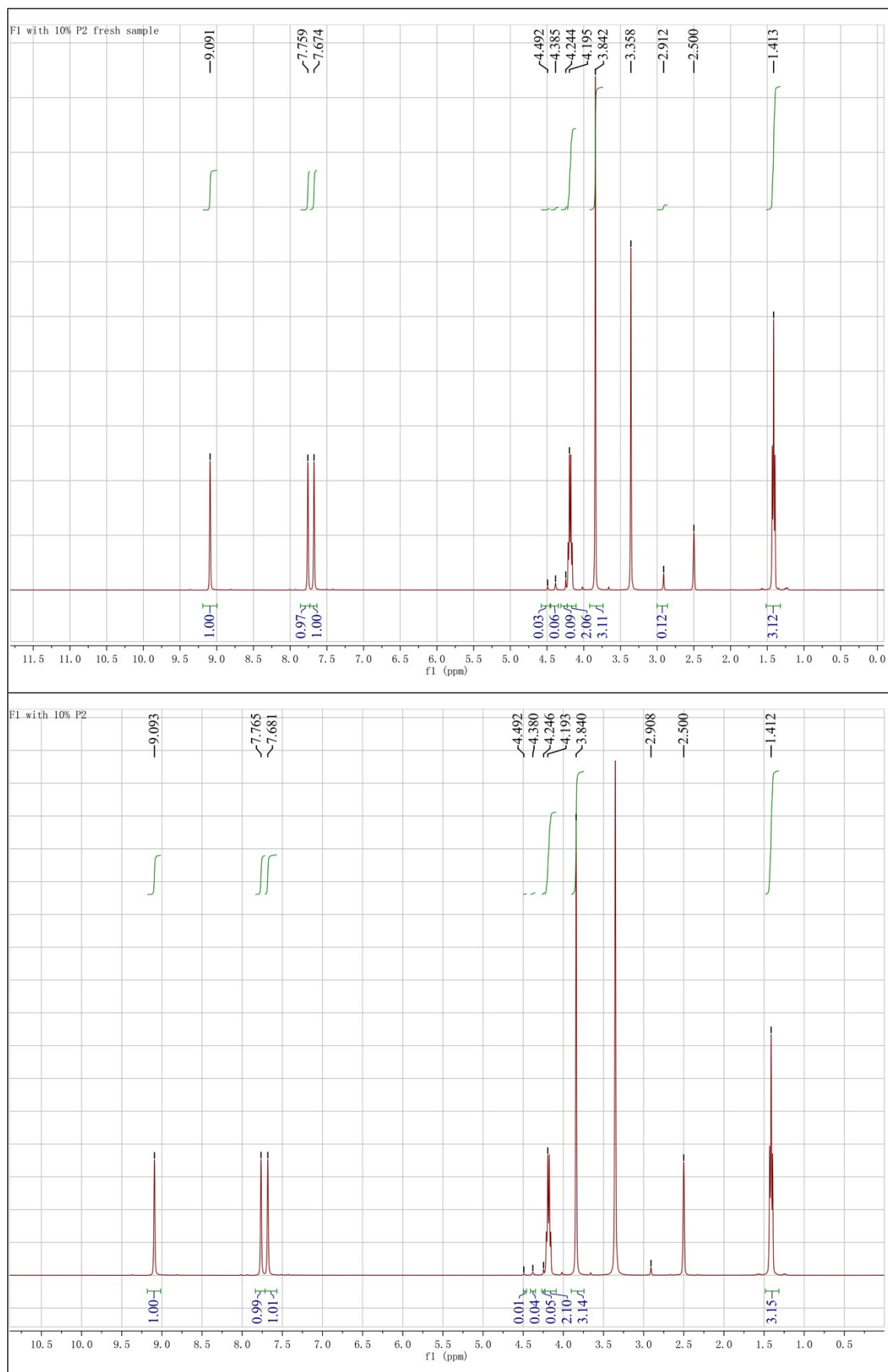


**Figure S12.**  $^1\text{H}$  NMR ( $\text{DMSO-}d_6$ ) of EIL fuel **F1** with 10 wt.% of promoter **P2**. (*top*): Before  $[t_0]$  and (*bottom*): after heating at  $50^\circ\text{C}$  for 7 days.

## Heats of Formation

To obtain the gas state heat of formations of the promoters, geometric optimization and frequency analyses were completed by using the M062X functional and a mixed basis set of SDD for Fe, Cu, I and 6-31+G(d, p) for other atoms (C, H, N, O and so on). Single energy points were calculated at the MP2 level and a mixed basis set of SDD for Fe, Cu, I and 6-311++G\*\* for other atoms. For the cations and anions, the optimized structures were characterized to be true local energy minima on the potential-energy surface without imaginary frequencies. Heats of formation (HOF,  $\Delta_f H^\circ$ ) of promoters were calculated based on a Born–Haber energy cycle (Figure S13).

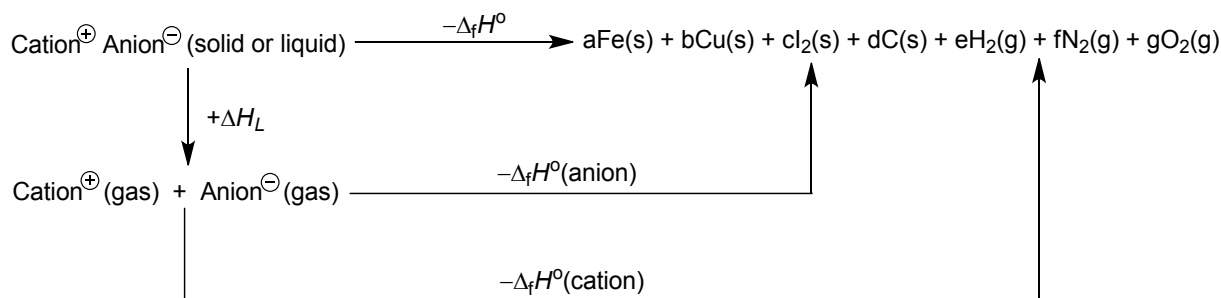


Figure S13. Born–Haber cycle for the formation of the promoters; the number of moles of the respective products are given by a, b, c, d, e, f, and g.

The solid state heat of formation for the promoters were calculated by the following equation. <sup>[R1]</sup>

$$\Delta_f H^\circ(\text{solid}, 298\text{k}) = \Delta_f H^\circ(\text{cation}, \text{gas}, 298\text{k}) + \Delta_f H^\circ(\text{anion}, \text{gas}, 298\text{k}) - \Delta H_L$$

The lattice energy  $\Delta H_L$  can be estimated using the DFT method with the GGA-RPBE (revised Perdew-Burke-Ernzerhof) exchange-correlation functional in Dmol3 program. <sup>[R2]</sup> The gas state heat of formation for the promoters, the component cations and anions were directly calculated by using the atomization method at MP2/SDD-6-311++G(d, p)// M062X/SDD-6-31+G(d, p) according to the literature methods. <sup>[R3]</sup> The calculation results of the promoters were shown in Table S1.

**Table S1.** The heats of formation data of the promoters.

sample	$\Delta_f H^\circ(\text{cation}, \text{gas}, 298\text{K})$ (kJ mol <sup>-1</sup> )	$\Delta_f H^\circ(\text{anion}, \text{gas}, 298\text{K})$ (kJ mol <sup>-1</sup> )	$\Delta H_L$ (kJ mol <sup>-1</sup> )	$\Delta_f H^\circ(\text{solid}, 298\text{K})$ (kJ mol <sup>-1</sup> )
Promoter 1	1102.19	-592.15	-209.55	1821.78 kJ mol <sup>-1</sup> /1.58 kJ g <sup>-1</sup>
Promoter 2	1102.19	-1050.97	-362.74	1516.15 kJ mol <sup>-1</sup> /0.99 kJ g <sup>-1</sup>

The heat of formation for the ionic liquid fuels, which used in this work, were obtained from the literature, <sup>[R4]</sup> and the data are shown in Table S2.

**Table S2.** The heats of formation of the fuels.

	F1	F2	F3	F4
$\Delta_f H^\ominus$	215.7 kJ mol <sup>-1</sup> / 1.22 kJ g <sup>-1</sup>	218.16 kJ mol <sup>-1</sup> / 1.44 kJ g <sup>-1</sup>	336.6 kJ mol <sup>-1</sup> /2.06 kJ g <sup>-1</sup>	-456.6 kJ mol <sup>-1</sup> / -1.95 kJ g <sup>-1</sup>

To the promoter-in-fuel mixtures, the heat of formations were calculated by a simple mathematical operation based on the ratio of fuel and promoters (Fuel-to-Promoter ratio = 9:1).

**Table S3.** The heats of formation of the fuel-promoter formulations.

	F1-P1	F1-P2	F2-P1	F2-P2	F3-P1	F3-P2	F4-P1	F4-P2
$\Delta_f H$ (kJ g <sup>-1</sup> )	1.26	1.20	1.45	1.40	2.01	1.95	-1.60	-1.66

## References

- [S1] L. A. Curtiss, K. Raghavachari, G. W. Trucks, J. A. Pople, *J. Chem. Phys.* 1991, 94, 7221–7230.
- [S2] (a) B. Delley, *J. Chem. Phys.* 1990, 92, 508-517; (b) B. Delley, *J. Chem. Phys.* 2000, 113, 7756-7764.
- [S3] (a) H. D. B. Jenkins, H. K. Roobottom, J. Passmore, L. Glasser, *Inorg. Chem.* 1999, 38, 3609–3620; (b) B. M. Betsy, E. F. C. Byrd, W. Mattson, In *Structure and Bonding, High Energy Density Materials*, (Ed.: T. M. Klapötke), Springer, Berlin, 2007, pp. 153 – 194.
- [S4] (a) Y. Wang, S. Huang, W. Zhang, T. Liu, X. Qi, Q. Zhang, *Chem. Eur. J.*, 2017, 23, 12502-12509; (b) Q. Zhang, P. Yin, J. Zhang, J. M. Shreeve, *Chem. Eur. J.*, 2014, 20, 6909-6914; (c) T. Liu, X. Qi, B. Wang, Y. Jun, C. Yan, Y. Wang, Q. Zhang, *Chem. Eur. J.*, 2018, 24, 10201-10207.